Carbohydrate Polymers 94 (2013) 235–243

Contents lists available at SciVerse ScienceDirect

Carbohydrate Polymers

journal homepage: www.elsevier.com/locate/carbpol

Effect of castor oil enrichment layer produced by reaction on the properties of PLA/HDI-g-starch blends

Zhu Xiong, Lisheng Zhang, Songqi Ma, Yong Yang, Chuanzhi Zhang, Zhaobin Tang, Jin Zhu*

Ningbo Key Laboratory of Polymer Materials, Ningbo Institute of Material Technology and Engineering, Chinese Academy of Sciences, Ningbo, Zhejiang 315201, PR China

ARTICLE INFO

Article history:
Received 19 August 2012
Received in revised form
29 November 2012
Accepted 17 January 2013
Available online 25 January 2013

Keywords:
Polylactide
Starch
Hexamethylenediisocyanate
Castor oil
Blends

ABSTRACT

Blends of entirely bio-sourced polymers, namely polylactide (PLA) and starch, have been melt-compounded by lab-scale co-extruder with castor oil (CO) as a plasticizer. The enrichment of castor oil on starch had great effect on the properties of the blends. If the castor oil was mainly dispersed in PLA matrix, the properties of the blends were poor, but when the hexamethylenediisocyanate (HDI) was grafted on starch granules the ready reactions between the hydroxyl on CO and the isocyante on the HDI-grafted starch (HGSTs) brought CO molecules enriched on starch particles. DSC analysis shows that the CO layer on starch has a positive effect on the crystallization of PLA in the ternary blend. The accumulation of CO on starch greatly improves the toughness and impact strength of PLA/starch blends. The grafting content of HDI on the starch granules primarily determined the compatibility and properties of the resulted blends.

1. Introduction

In recent years, environmental concerns and shortage of petroleum resources have driven efforts on development and production of biodegradable and renewable materials, which are known as "green materials" (Bledzki & Sperber, 1999). Poly(lactic acid) (PLA) is one kind of biodegradable aliphatic polyester with excellent properties for various applications, which will play a major role in the future markets for polymers from renewable resources. However, the disadvantages of brittleness and high cost of PLA limit PLA's wide spread applications (Anderson, Schreck, & Hillmyer, 2008; Auras, Harte, & Selke, 2004). Thus, in order to resolve these two problems, plasticizers and cheap fillers were needed to add into PLA's matrix (Huda, Drzal, & Misra, 2006; Jacobsen, Fritz, & Degee, 2000). To reduce the cost, starch, as a common and inexpensive biopolymer, is an attractive candidate as organic filler for PLA. PLA/starch blends were well-explored biodegradable materials. Nevertheless, PLA and starch are thermodynamically incompatible (Wang, Sun, & Seib, 2001). Obviously, the incorporation of native starch into PLA could increase its rigidity but at the same time greatly reduced elongation at break (EB) and the impact strength (IS) (Jacobsen & Fritz, 1999; Ke & Sun, 2003).

Many factors were believed to cause the deterioration in mechanical properties of PLA/starch blends. Firstly, PLA is a material with inherent brittleness. Earlier research has reported that the mechanical properties of PLA are similar to that of polystyrene (Anderson et al., 2008; Bhardwaj & Mohanty, 2007) and like polystyrene, one of the deficiencies of the material is its brittleness, as evidenced by relatively low tensile strain at break, toughness, and impact strength. Secondly, native starch is of rigid granular structure as well as the particle diameter ranging from 10 to 200 μm (Dhital, Shrestha, & Flanagan, 2010), which would further increase the intrinsic brittleness of PLA (Jiang et al., 2002). Furthermore, the interfacial adhesion between hydrophobic PLA and hydrophilic starch is very poor. Obviously, the starch particles dispersed in PLA matrixes act as the defects and lead to serious stress concentration, which makes the material fractured more easily.

When attempting to improve the mechanical properties of PLA, research has mainly focused on two methods. One is the use of reactive compatibilizers or coupling agents. Interfacial adhesion plays a vital role in mechanical properties of polymeric composites. Reactive interfacial coupling agents are often used to improve interfacial properties and control morphologies of polymeric composites. Coupling agents containing reactive functional groups such as maleic anhydride (MA) (Zhang & Sun, 2004), acrylic acid (AA) (Wu, 2005) and methylene-diphenyldiisocyanate (MDI) (Wang et al., 2001) are able to generate in situ formation of blocks or grafted copolymers at the interface by hot-melting blending. However, all above referred coupling agents used in PLA/starch blends are inefficient on the improvement of toughness.

Another method to improve the mechanical properties of PLA/starch blends is gelatinizing of starch. Thermoplastic starch

* Corresponding author. Tel.: +86 574 86685925; fax: +86 574 86685925.
E-mail address: jzhu@nimte.ac.cn (J. Zhu).

0144-8617/$ – see front matter © 2013 Elsevier Ltd. All rights reserved.
http://dx.doi.org/10.1016/j.carbpol.2013.01.038

(TPS) was prepared by inserting small molecule plasticizer into the polysaccharides crystalline of starch. The commonly utilized plasticizers include water (Teixeira et al., 2007), glycerol (Rodriguez-Gonzalez, Ramsay, & Favis, 2004), urea (Ma, Yu, & Wan, 2006) and citric acid (Shi et al., 2007). Although, in a melting blend process, the strong intermolecular hydrogen bond is broken and replaced by intra-molecular hydrogen bond between polysaccharide chains and low molecular weight plasticizer resulted in a much finer dispersed phase size in PLA matrixes, the small molecule plasticizer may cause gradation of PLA during processing. What is more, TPS is an unstable system and the retrogradation of starch crystalline and the migration of the plasticizer can cause aging of the product and deteriorate the mechanical properties.

To prevent the migration of the small plasticizers, chemical bond can be generated between the plasticizers and the starch. Wang (Wang, Zhai, & Zheng, 2012) caped polyethylene glycol (PEG), a plasticizer, with MA and then grafted this MA–PEG–MA onto the native starch. This modified starch was then blended with PLA and more PEG plasticizer from an extruder. The resultant compound showed good compatibility between MA–PEG–MA modified starch and the PLA as well as the mechanical properties. However, the used plasticizer PEG was derived from petrochemical resource.

Recently, bio-based plasticizers have attracted the general attention due to their renewability. A series of studies have been done by Hillmyer's group on the utilization of triglyceride oils as toughening agents for PLA (Chang, Robertson, & Hillmyer, 2009; Gramlich, Robertson, & Hillmyer, 2010; Robertson et al., 2010; Robertson, Paxton, & Hillmyer, 2011). The oils do not toughen the PLA matrix; rather, the PLA and oil form a phase separated mixture. So, the PLA/starch blend would be more difficult to be plasticized by oil in contrast with neat PLA. The mechanism of toughening in PLA/starch blends can be interpreted by a flexible interphase layer toughening brittle polymers (Wang et al., 2012). Our motivation for using triglyceride oils is to create a toughened PLA/starch composites (analogous to the flexible interphase layer toughening techniques used to produce high-ductility PLA/starch blends) derived entirely from renewable resources. Though other studies have shown that the tensile and impact toughness of PLA/starch blends can be improved by the formation of plasticizer-rich interphase layer on the surface of starch blends, the blending plasticizers used were derived from petroleum.

This paper follows our previous paper on the utilization of epoxidized soybean oil as the reactive toughening agent for PLA/starch blends (Xiong, Yang, & Feng, 2013). The epoxidized soybean oil do not directly plasticize the PLA/starch blends well. But, when the maleic anhydride (MA) was grafted on starch granules via organic solution reaction, the ready reactions between the epoxy on ESO and the carboxyl on the MA-grafted starch (MGST) brought ESO molecules enriched on starch particles. The plant oil layer significantly improved the compatibility and mechanical properties of the resulted blends.

In this work, we focus on castor oil, a triglyceride containing the hydroxyl bearing ricinoleic acid as 90% of its fatty acids (Guner, Yagci, & Erciyes, 2006). Castor oil as a raw material for polymers has found applications in polyamides (such as Nylon-11) (Nayak, 2000), polyurethanes (Petrovic et al., 2008), and interpenetrating networks (Sperling & Mishra, 1996). To evaluate the efficacy of castor oil as a renewable resource blending component for PLA/starch blend, we explored the morphology, thermal, mechanical and rheology properties of PLA/starch blends containing 5 wt.% castor oil.

The utilization of diphenylmethanediisocyanate (HDI) as to improve the properties of incompatibility PLA/starch blends has been well established in the literature (Wang et al., 2001). To further enhance the compatibility of ternary blends of PLA, starch and castor oil, we explored the use of hexamethylenediisocyanate (HDI) to control the blend morphology and improve the interfacial adhesion of starch with castor oil. Building upon the work of Pan (Pan et al., 2011), we synthesized HDI-grafted starch containing isocyanate groups. Blends containing PLA, castor oil, and modified starch granules were subsequently prepared and analyzed. The anchored castor oil on the starch in the different tenary blends was determined and its effect on thermal, mechanical properties and rheological characterization was thoroughly investigated. The resulting fractured surfaces and crystal growth were observed with scanning electron microscopy (SEM) and optical micrographs, respectively.

2. Experiment

2.1. Materials

The PLA 4032D, a semi-crystalline extrusion grade, was supplied by NatureWorks (Minnesota, USA). It was vacuum dried at 80 °C at least 8 h prior to use. The native food grade corn-starch was obtained from the Zhucheng Stimulation Trade and Corn Development Limited Company, Shangdong, China, which was dried in a vacuum dryer for 24 h at 100 °C before use. The chemical pure (CP) grade castor oil (CO), 99% HDI and analytical pure (AR) grade toluene were purchased from the Aladdin Reagent (Shanghai, China) and used directly without further purification.

2.2. Synthesis of HDI-grafted starch

In a three-necked flask equipped with an oil-and-water separator, a condenser tube and a mechanical agitator, were added 200 mL toluene, 100 g of starch and a certain amount of HDI with ditin butyl dilaurate (DBTDL) as a catalyst to improve the reactivity of core-starch with HDI. The agitation was kept for 5 h at 60 °C. Subsequently, the reaction was cooled to room temperature and washed with acetone by six times to remove residual HDI and toluene. Finally, the product was obtained after filtration and dried in the vacuum oven for 24 h at 60 °C. The final products were preserved in desiccating dryer for further characterization. The reaction is illustrated in Fig. 1. Three types of HDI-grafted starch (HGST) were obtained with HDT at 5 wt.%, 8 wt.% and 11 wt.% of starch denoted as HGST1, HGST2 and HGST3, respectively. The chemical structures of different HGSTs were characterized by FTIR (Nicolet FTIR 6700 infrared spectrophotometer, KBr powder) over a range of 4000–400 cm^{-1}.

2.3. Preparation of the blends

The PLA/starch, PLA/CO/starch, and PLA/CO/HDI-graft-starch blends were firstly melt-blended in a SJSZ-10A miniature twin screw extruder (Ruiming Plastics Machinery, Wuhan, China). The rotation rate, mixing temperature and time were set at 40 rpm, 175 °C and 5 min, respectively. Where-after, the PLA blends were extruded into an SZ-15 micro-injection molding machine made by Ruiming plastic Machinery. All the standard test bars for various measures were prepared under an injection pressure of 5 MPa for 30 s at 200 °C with mold temperature of 40 °C. In the PLA/starch, PLA/CO/starch, and PLA/CO/HDI-graft-starch blends, the content of starch was 30 wt.%. In the PLA/CO/starch and PLA/CO/HDI-graft-starch blends, the addition of CO was 5 wt.%. Meanwhile, the HDI-graft-starch with different grafting ratios was also investigated in the PLA/CO/HDI-graft-starch blends (65/5/30).

2.4. Morphological characterization

The morphology of the blends was recorded in a low expansion scanning electron microscope (SEM, Hitachi TM-1000). The

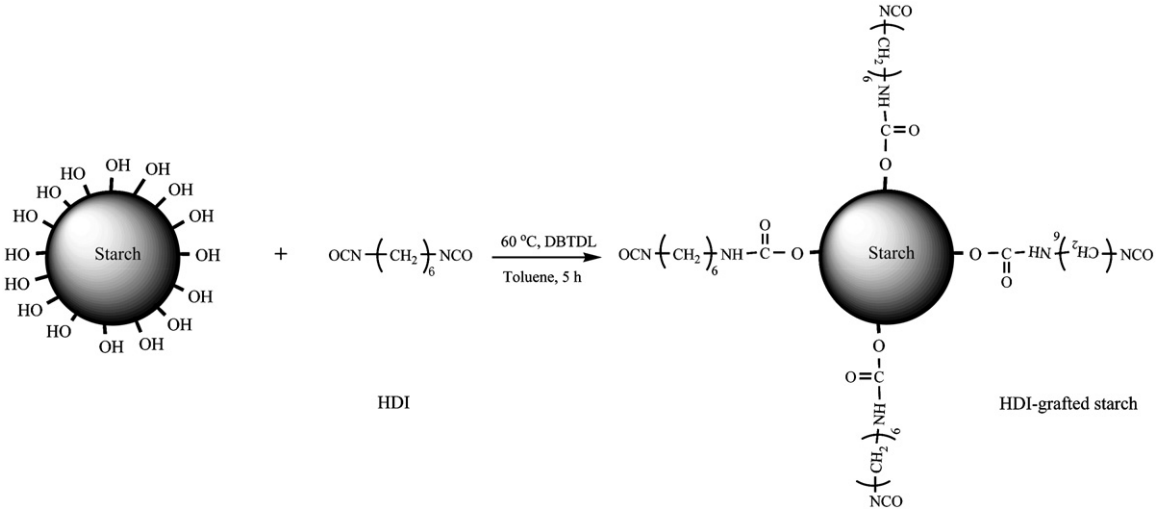

Fig. 1. The grafted reaction of native starch granule with HDI.

samples were fractured in liquid nitrogen. The resulting fractured surfaces were sputtered with gold prior to examination.

2.5. Thermal analysis

The thermal properties of the blends were characterized by differential scanning calorimetry (DSC) on a Pyris Diamond DSC instrument. The samples were stabilized at 30 °C for 1 min before there were heated to 200 °C at 10 °C/min and then the samples were held at 200 °C for 5 min to erase thermal history prior to cooling down to 30 °C at 25 °C/min. After 1 min at 30 °C, the second scan from 30 °C to 200 °C at 10 °C/min was performed. Throughout the whole process, the sample cell was kept under a nitrogen flow of 20 mL/min. The glass transition temperature (T_g), crystallization temperature (T_c), and melting temperature (T_m) were determined from the second scan.

The glass transition temperature (T_g), crystallization temperature (T_c), melting temperature (T_m), and degree of crystallinity (χ_c) were determined from the second heating scan. T_m and T_c were taken as peak values, and T_g was taken as the midpoint of heat capacity changes. When multiple endothermic peaks were obtained, the peak temperature of the main endotherm was taken as T_m. The degree of χ_c is defined as the enthalpy difference between melting and crystallization peaks divided by the enthalpy of 100% crystalline PLA (93.6 J/g) according to Eq. (1) (Fischer, Sterzel, & Wegner, 1973)

$$\chi_c(\%) = \frac{(\Delta H_m + \Delta H_c) \times 100}{93.6 \times \chi_{PLA}} \quad (1)$$

where ΔH_m and ΔH_c are the enthalpies (J/g) of fusion and crystallization of the blend, respectively; 93.6 J/g is the enthalpy of fusion of a PLA crystal of infinite size; and χ_{PLA} is the PLA content. All samples were tested in triplicate.

2.6. Polarized optical microscopy (POM)

Optical microscopy was then carried out under polarized light to observe the formation and size of the spherulitic crystal. All microscopic observations were made with a polarizing microscope (POM, Olympus BX51) between crossed polar. The temperature control of a sample was performed using a hot stage (Linkam TH-600PM, Linkam Scientific Instruments, UK). The temperature of the apparatus was at 115 °C. PLA resin sandwiched between microscope glass slides was heated to 200 °C on a hot plate and was pressed with small stress to prepare thin film samples with desired thickness. The morphology of the thin film sample between the glass slides was observed on a hot stage and recorded on a hard disk.

2.7. Measurements of mechanical properties

An Instron 5567 (Wuhan, China) was used for the mechanical property measurements following the GB/T 1040.1-2006. System control and data analysis were performed using the instrument software. The standard oar-shaped samples were used in order to determine the tensile strength (TS), tensile modulus (E) and elongation at break (EB). Four samples for each composite were tested at a cross head speed of 20 mm/min. The impact test was performed according to ISO179-1: 98. A 5.5 J pendulum was used to determine the Charpy impact strength, the dimension of bar samples was 80 mm × 10 mm × 4 mm. The impact testing was performed on a mechanical impact tester (XJ-50Z, Chengde Dahua Testing Machine Co. Ltd., Chengde, China). Four samples for each composite were tested.

2.8. Rheological characterization

The rheological behavior of the samples was studied by dynamic oscillation made using a dynamic analyzer Physica MCR-301 of Rheometric (Anton Paar, Austria) with parallel plate tools. The plate diameter and its gap were 25.0 mm and 1 mm, respectively. The dynamic frequency sweep was carried out from 1 to 100 rad/s at 180 °C with strain of 1%. The all samples used for the rheological behavior characterize came from extruded samples.

3. Result and discussion

3.1. The FTIR analysis of HGST with various amount of HDI

The isocyanate (—NCO) groups were immobilized onto the surfaces of the starch nanoparticles by the reaction between surface hydroxyl (—OH) groups of the native starch and one isocyanate group of HDI (Fig. 1). Fig. 2 shows the FTIR spectra of HGST with various amount of HDI. Although the amide group characteristic of HGSTs at 1635 cm^{-1} (C=O stretching) overlapped with native starch, the —NH bending characteristic peak at 1565 cm^{-1} was clearly shown on HGSTs. Meanwhile, the peak at 2270 cm^{-1} (—NCO of HDI) was found in the FTIR spectrum of the HDI-grafted starch (HGDT). The intensity of —NCO peaks increased with increasing

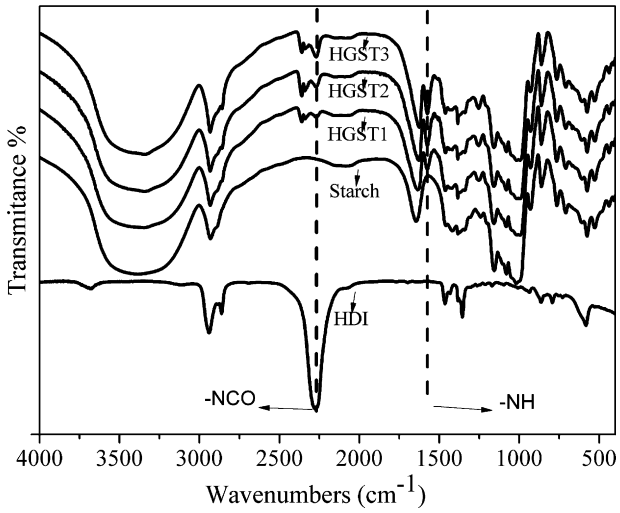

Fig. 2. The FTIR spectra of HGST with various amount of HDI.

the amount of HDI. This indicated that the NCO grafted starch was obtained.

3.2. Morphology

The fractured surfaces of PLA/native starch blend (70/30), PLA/HGST1 blend (70/30), PLA/native starch/CO blend (65/30/5) and PLA/CO/HGST blend (65/5/30) with different HDI grafting ratios in MGSTs were examined by SEM and showed in Fig. 3. A clear gap between PLA matrix and the native starch granules was seen, showing no compatibility between PLA and the native starch (Fig. 3a). When PLA, native starch and CO mixed with the ratio of 65/30/5 were melt blended together, CO could not improve the compatibility between PLA and the native starch to an extent that many clear gaps between the two phases were found in Fig. 3c. Meanwhile, CO is seen as scattered macro-droplets within the PLA matrix, indicating that the interacting between starch particles and CO was poor and resulted in the CO molecules mainly dispersing in PLA matrix.

The SEM image of PLA/HGST1 blends is shown in Fig. 3b and less gaps were observed, indicating the end carboxyl groups (—COOH) or hydroxyl groups derived from PLA have reacted with the isocynate groups originated from HGST1 as a result of good compatibility between PLA and HDI-grafted granules, similar results also obtained by (Yu et al., 2011). Meanwhile, with the weight of 5% CO in PLA/HGST1 blend, in Fig. 3d, it could be observed that the size of CO macro-droplets in PLA matrix was decreased in comparison with PLA/starch/CO ternary blend, but the compatibility of HGST1 with the PLA matrix in the tenary blend was poorer than PLA/HGST1 binary blend. According to Robertson's research (Robertson et al., 2011), the size of CO droplets in PLA matrix would become smaller with decreasing content of CO or the addition of compatibilizer. Whereas, there were no other compatibilizers and the content of CO was unchanged in PLA/HGST1/CO blend. Thus, it was supposed that some CO molecules have reacted with HGST1 and been capped on the surface of HGST1 particles, which made the content of CO in the PLA matrix decrease. That was why the size of CO droplets in the tenary blends was decreased. On the other hand, the isocyanate groups of HGST1 would react with hydroxyl groups of CO prior to hydroxyl groups at the end of PLA due to CO's higher reactivity (Zhong et al., 1999). This caused the poor compatibility of HGST1 particles with PLA matrix.

Fig. 3e and f shows PLA/HGST/CO blends with increasing grafting levels of HGSTs. They showed that the compatibility between PLA and the starch was improved with more content of HDI, since more blurring interface was found in Fig. 4f. The number of CO droplets was also gradually decreased in the PLA matrix with increasing the content of HDI. Thus, it was concluded that the introduction of more isocyanate groups onto the starch surface would not only improve its reactivity with CO, but have the excess isocynate groups (—NCO) to react with the end carboxylic acid groups (—COOH) or hydroxyl groups on PLA, resulting in a compatible blend of PLA, HGST and CO. For example, in the PLA/HGST3/CO (65/30/5) blend, almost all CO molecules were located around the grafted starch granule, schematized in Fig. 4.

3.3. Thermal properties

As shown in Table 1, the pure PLA shows a small the glass transition at 61.8 °C (T_g), an exothermic cold crystallization peak at 117 °C (T_c) and a sharp endotherm peak at 164 °C with a shoulder peak to its right (Fig. 7 in supplementary data). This phenomenon of PLA was reported to be a result of lamellar rearrangement during crystallization of the polymer as well as the reorganization of poor crystalline regions with different crystalline structures within PLA (Martin & Averous, 2001; Nijenhuis et al., 1996). Similar thermal properties were observed for PLA/Native starch (70/30) blend. In contrast to native starch, after starch grafted by HDI, T_g was slightly increased from 60.7 °C to 62.6 °C, whereas T_c decreased by nearly 8 °C in comparison with the pure PLA. Sorenson (Sorenson, 1959) had found that a mixed carbamic–carboxylic anhydride could be produced via the reaction of an isocyanate group (—NCO) with carboxylic acid (—COOH) as a result of reduced chain mobility of PLA in melt-blend process. Whereas, the improved compability of starch particle with PLA matrix might induce the lamellar rearrangement and accelerate the crystallization rate of PLA matrix resulted in the T_c decreasing. But, the χ_c of PLA/HGST1 was only 2.7%, indicating that the induced crystallization of starch particles on PLA was limited, also confirmed by (Tianyi & Sun, 2003).

To determine if the CO has an effect towards thermal behavior of PLA/native starch blends, the PLA/native starch/CO blend was prepared by the melt-blended mixer. As shown in Table 1, it was observed that T_c of PLA/native starch decreased from 114 °C to 106 °C with CO. Meanwhile, the lower T_m peak obviously declined, indicating that CO facilitated the forming of the crystalline corresponding to the higher T_m peak in PLA/native starch system. Whereas, the T_g of PLA/native starch blends unchanged with CO, was about 60.6 °C. The major reason was that the CO was dispersed in the PLA matrix with macro-droplets. Thereof, the CO could not function as a plasticizer to enhance the chain mobility and decrease the T_g of PLA. However, the CO could induce the crystallization of PLA depending on hydrogen bonding of CO molecules. The similar phenomenon about hydrogen bonding induced PLA crystallization has been reported by Lin (Lin et al., 2007). But, the effect of CO's hydrogen bonding on the PLA crystallization was weak. Meanwhile, it was seen that the crystallization degree (χ_c) of PLA/starch/CO (65/30/5) blend was only increased to 3.1%.

According to Table 1, HDI grafted starch significantly changed the thermal behavior of PLA/starch/CO. The major changes were that, with HGST1, T_c decreased from 106 °C to 100 °C, and the χ_c obviously increased from 3.1% to 10.3%. This may be explained by that the functional groups on the HDI grafted starch reacted with CO and formed many long grafting chain structure containing amide groups (—NH—CO—) on the surface of starch granules. From our group's previous and Xing's researches (Tang et al., 2012; Xing et al., 2012), the hydrogen bond interaction between amide groups (—NH—CO—) and the carbonyl groups in PLA was proposed to be an important factor influencing the crystallization of PLA. Moreover, with the grafting ratio of HDI on the surface of starch increasing, the χ_c further increased due to more CO molecules enriching on the surface of HDI grafted starch granules as well as the amide groups (—NH—CO—). However, very few literatures

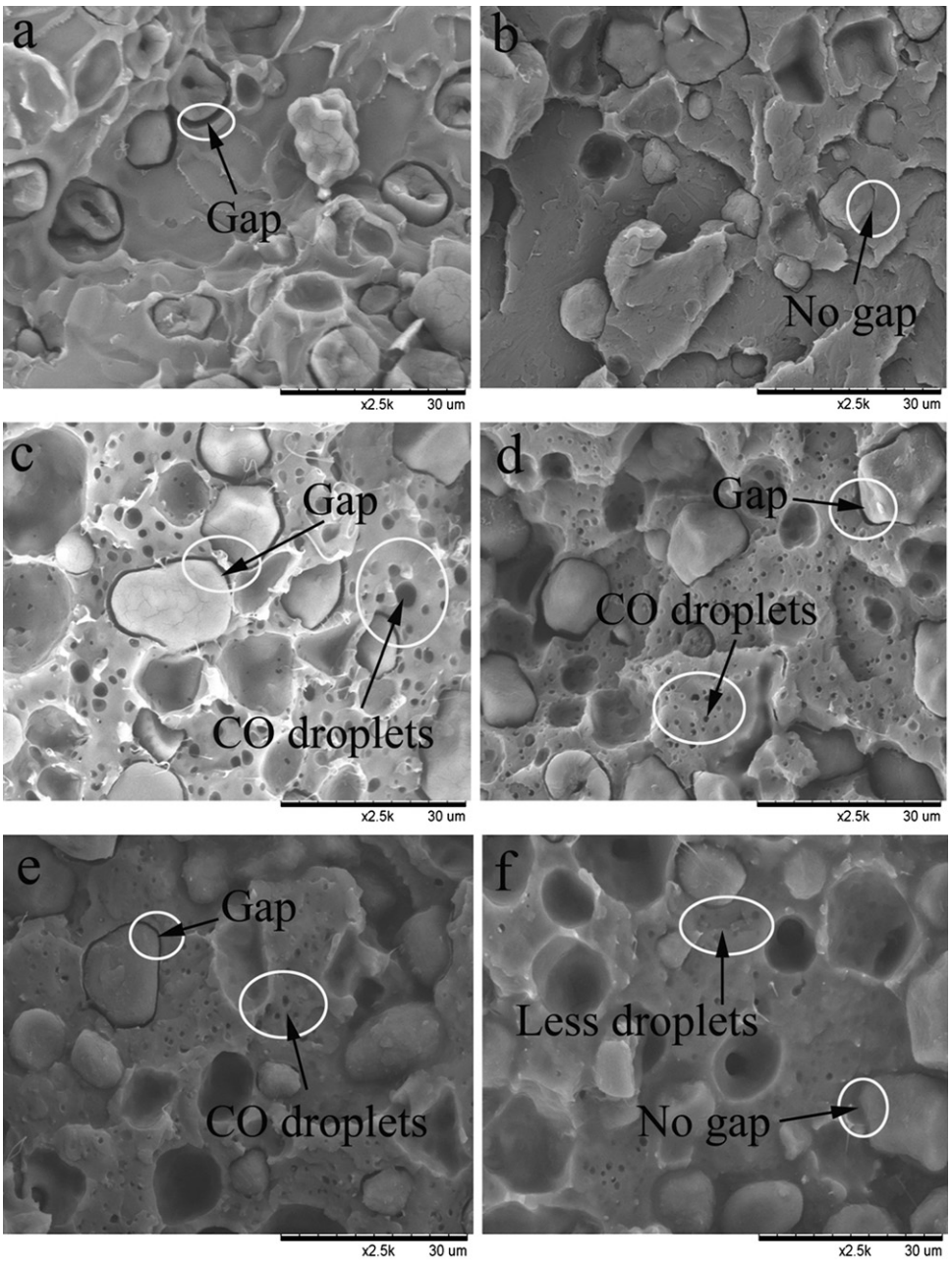

Fig. 3. SEM images of (a) PLA/native starch blend (70/30) and (b) PLA/HGST1 blend (70/30) and (c) PLA/native starch/CO blend (65/30/5) and (d–f) PLA/HGST/CO blend (65/30/5) with different HDI grafted ratio in MGST.

Table 1
Thermal properties of neat PLA, PLA/30 wt.% starch composite with or without 5 wt.%, PLA/HGST1 blend (70/30) and PLA/HGSTs/CO blends (65/30/5).

Compositions	T_g (°C)	T_c (°C)	ΔH_c (J/g)	T_{m1} (°C)	T_{m2} (°C)	ΔH_{m2} (J/g)	χ_c (%)
Neat PLA	61.8 ± 0.5	117 ± 3	−37.5 ± 0.8	164 ± 1	168 ± 1	–	–
PLA/NST (70/30)	60.7 ± 0.8	114 ± 3	−25.6 ± 0.5	164 ± 1	169 ± 1	20.4 ± 0.4	–
PLA/HGST1 (70/30)	62.6 ± 0.3	109 ± 1	−25.1 ± 0.3	160 ± 1	168 ± 1	26.9 ± 0.3	2.7 ± 0.3
PLA/NST/CO (65/30/5)	60.6 ± 0.5	106 ± 2	−20.3 ± 0.5	160 ± 1	167 ± 1	22.2 ± 0.5	3.1 ± 0.5
PLA/HGST1/CO (65/30/5)	61.3 ± 0.7	100 ± 1	−20.0 ± 0.7	–	165 ± 2	26.3 ± 1.0	10.3 ± 0.8
PLA/HGST2/CO (65/30/5)	61.0 ± 0.4	100 ± 2	−19.4 ± 1.2	–	166 ± 1	26.9 ± 0.8	12.3 ± 1.0
PLA/HGST3/CO (65/30/5)	61.2 ± 0.6	100 ± 2	−19.0 ± 1.0	–	166 ± 1	27.0 ± 1.0	13.1 ± 1.0

T_g, T_c, ΔH_c, T_{m1}, T_{m2}, ΔH_{m2} and χ_c represented glass transition temperature, cold crystallization temperature, crystallization enthalpy, low melt temperature, high melt temperature, high melt peak fusion enthalpy, and degree of crystallinity, respectively. "–" represents uncalculated value from Eq. (1).

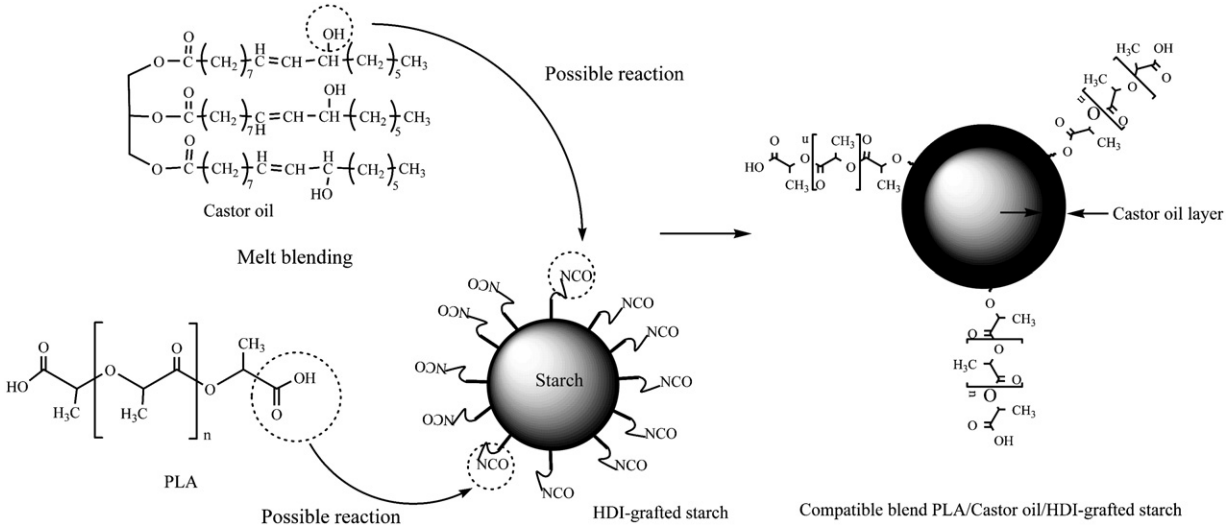

Fig. 4. The possible chemical reaction diagram in PLA/HGSTs blends with CO during melting blend process.

reported the crystallization of PLA facilitated by CO layer on the starch surface. Thus, the major reason needs to be further investigated by the future work (the DSC date of Table 1 was obtained from supplementary data Fig. 7).

3.4. Polarized optical microscopy (POM)

The effect of CO on the crystalline morphology of PLA/starch blends with or without HDI grafting was further observed with POM, and the results are shown in Fig. 5. At the beginning, we could find that starch particles, irrespective of HDI grafting, showed a white and bright spherical morphology in Fig. 5a and b. After isothermal crystallization at 115 °C for 6 min in Fig. 5a, the picture almost resumed its original form until up to 6 min. However, for PLA/HGST3/CO (65/30/5) blend (Fig. 6b), many spherulites formed by PLA matrix have appeared around the HGST3 granules at 115 °C for 2 min. Meanwhile, with increasing crystallization time at 115 °C, the nucleus density of crystallites was largely increased. The major reasons may be explained by the SEM, it was known that most of the CO molecules were accumulate on the surface of MGST3 granules forming a CO layer, but not for native starch particles. Thus, it was inferred that the CO layer on the starch surface enhanced the formation of PLA crystal nucleus.

3.5. Mechanical properties

The morphology changes brought up the change of the mechanical properties of the PLA/starch blends. Table 2 shows these changes. A pure PLA is a fairly rigid material with a high modulus (~3000 MPa) and tensile strength (~66 MPa), but quite brittle, with the elongation at break (EB) and impact strength of 5% and 18 kJ/m^2, respectively. The addition of native starch to PLA matrix caused a decrease in Young's modulus (~2700 MPa), tensile strength (~50 MPa) and impact strength (~10 kJ/m^2), which was caused by the weak compatibility between native starch particles and PLA matrix, but almost no effect on EB (~6%) was found. With 5 wt.% CO in PLA/starch blend, according to Table 2, all properties excepted for tensile strength of PLA/native starch/CO blend (65/30/5) were almost unchanged in comparison with PLA/native composite (70/30). Obviously, the CO could not function as a plasticizer to tune the PLA/native starch blend from rigid to ductile. This result was attributed to the weak reaction among the ternary components, observed in Fig. 3c.

As to the HDI grafted starch, the compatibility between PLA and the starch was greatly improved as a result of enhanced impact strength (~13 kJ/m^2) and tensile modulus (~2900 MPa), but the EB (~2%) was decreased. It was well known that, without any plasticizers, the good compatibility of starch with PLA would only enhance the PLA's stiffness due to the stiff structure of starch particles (Zhang & Sun, 2004). However, with 5 wt.% CO in PLA/HGST1 blend, the impact strength and EB were both significantly increased up to 25 kJ/m^2 and 45%, respectively, indicating that the CO could play a plasticizer in the PLA/HGST1 blend, but not for PLA/native starch blend. Meanwhile, with the increasing of HDI grafting on the starch surface, the EB and impact strength was increased as high as 68% and 41 kJ/m^2, respectively, in the blend of PLA/HGST3/CO (65/30/5). Therefore, the higher the grafting ratio of HDI in starch was, the higher the EB, tensile strength and the impact strength were. It was mainly due to the layer of CO on the starch.

Maybe, the good mechanical properties of PLA/HGSTs/CO (65/30/5) blends could be explained in terms of improved compatibility. Additionally, it may also be reasonable to assume that most of CO molecules might have been accumulated on the surface of the starch particles via the reaction between hydroxyl groups (—OH) and the isocynate groups (—NCO) of the HGSTs as a result of reduced amount of CO in PLA matrix in Fig. 3d–f, and the CO formed a flexible interface phase, which acted as craze terminators and caused the improvement of ductility in tensile process. Although the definite flexible interface phase on the surface of HGSTs could not be observed by SEM or TEM due to the large size of starch granules, the similar conclusion of interface transition layer formed by PEG between PLA matrix and starch via the reaction toughened the PLA/starch blend has been recently reported by Wang (Wang et al., 2012).

3.6. Rheological characterization

The rheology of polymers is very sensitive to changes of plasticizers in the melted blend process and is therefore of practical and fundamental interest in the current study. Fig. 6 presents the viscosity of PLA, PLA/starch blend, and PLA/starch blends/CO with and without HDI grafting at a temperature of 180 °C. The data of neat PLA were obtained from oscillatory measurement carried out on the non-extruded pellets. It exhibited a clear Newtonian Plateau with a zero-shear 993 Pa.s. With 30 wt.% starch, it also showed a clearly defined Newtonian region but the zero-shear viscosity is decreased to 480 Pa.s, 2-fold decrease when compared to the neat PLA.

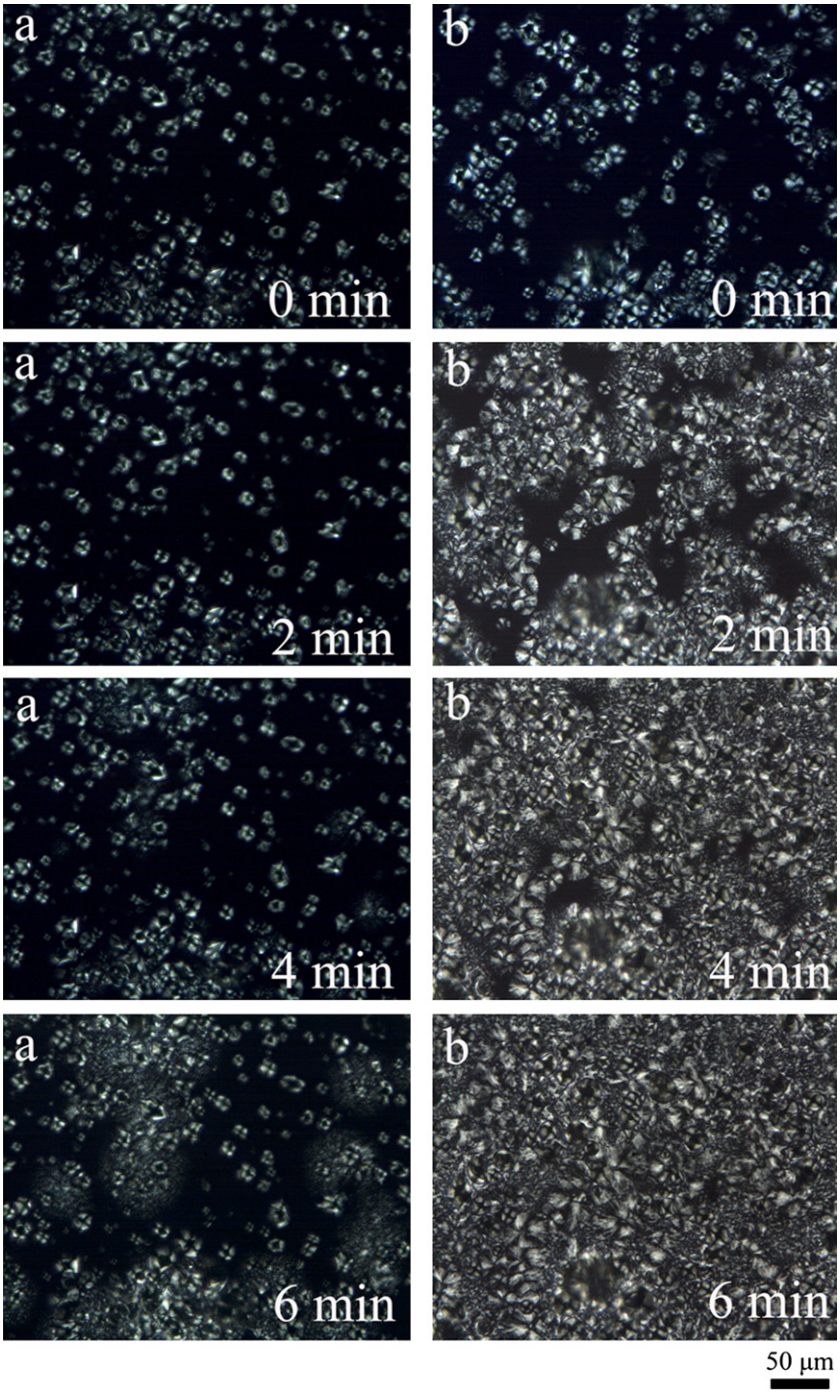

Fig. 5. the POM of PLA/starch/CO (65/30/5) blend (a) and PLA/HGST3/CO (65/30/5) blend (b) at 115 °C isothermal crystallization for 6 min.

Table 2
The mechanical properties of neat PLA and PLA/30 wt.% starch blends with or without 5 wt.% CO, PLA/HGST1 composite (70/30) and PLA/HGSTs/CO blends (65/30/5) with various HDI grafted ration in starch.[a]

Composite	IS (kJ/m^2)	TS (MPa)	EB (%)	TM (MPa)
Pure PLA	18(±2)	65(±3)	5.0(±1)	3000(±20)
PLA/starch (70/30)	10(±1)	50(±1)	6.0(±1)	2700(±30)
PLA/HGST1 (70/30)	13(±1)	42(±1)	2.5(±1)	2900(±50)
PLA/starch/CO (65/30/5)	11(±1)	40(±1)	7.0(±1)	2850(±80)
PLA/HGST1/CO (65/30/5)	25(±2)	28(±1)	45(±5)	2530(±60)
PLA/HGST2/CO (65/30/5)	32(±1)	31(±2)	50(±5)	2450(±50)
PLA/HGST3/CO (65/30/5)	41(±2)	33(±1)	68(±5)	2500(±70)

[a] Values reported here are averages of four tensile bar tests according to the test standard. IS, TS, EB and TM represented the impact strength, tensile strength, elongation at break and tensile modulus, respectively.

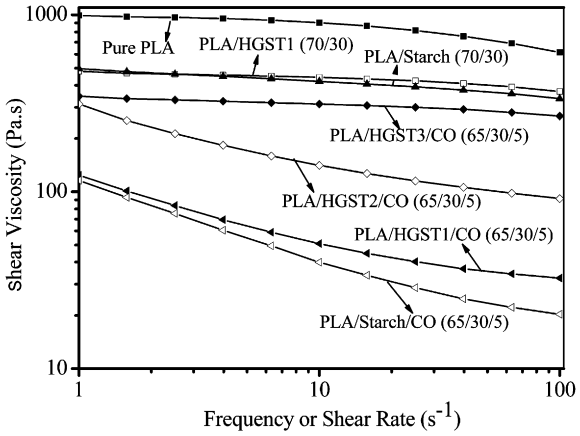

Fig. 6. Viscosity of neat PLA, PLA/starch with or without HDI grafting, PLA/starch/CO and PLA/HGSTs/CO blends.

Similar rheological curve was observed by the PLA/HGST1 blend, but slightly higher than that of PLA/starch blend with the increasing shear rate resulted from the formation of crosslink unit between starch and PLA matrix, also observed by Xie (Xie et al., 2007).

In order to make clear the effect of CO on the rheological property of PLA/starch with and without HDI grafting, the viscosity of PLA/starch blends with 5 wt.% CO is presented in oscillatory shear and the measurement was limited to the 1–100 s^{-1} frequency range to limit the duration of the measurement. In Fig. 6, it was observed that the viscosity of PLA/native starch blend with 5 wt.% CO was about 116 Pa.s, which was significantly lower than that of PLA/native starch blend. Meanwhile, the viscous behavior of PLA/native starch/CO (65/30/5) blend was very different from that of PLA/starch blend. The PLA/native starch/CO (65/30/5) blend did not exhibit any viscosity plateau in the range of investigated shear rate and was highly shear thinning. Obviously, the CO existed in the PLA matrix could significantly decrease the PLA's melt viscosity.

As to the HDI grafted starch, it was found that the zero-shear viscosity was increased up to 330 Pa.s with the HDI grafting ratio increasing on the starch particles, and the viscous behavior was gradually changed, especially for PLA/HGST3/CO blends. The viscous behavior was similar to that of PLA/starch blend and presented a Newtonian Plateau. Obviously, it could be supposed that the amount of CO existed in the PLA matrix was reduced and more CO molecules were accumulated on the surface of starch granules via the reaction, which resulted in the difference of melt viscous behavior from PLA/starch or PA/HGST1 blends.

4. Conclusions

Castor oil (CO) could not be used as a bio-based reactive plasticizer for PLA and the starch, but this effect was changed by chemically grafting hexamethylenediisocyanate (HDI) on the starch granules. Through the SEM analysis, the ready reactions of isocyanate groups on HDI-grafted starch (HGSTs) with the hydroxyl groups on CO and the end carboxylic acid groups of PLA brought the components of this blend together and formed a CO layer on the surface of starch. The characterization of the obtained blends by differential scanning calorimetry (DSC) demonstrated that the cold crystallization temperature (T_c) of PLA was obviously declined by the formation of CO layer via the reaction of HGSTs with CO on the surface of HGSTs particles. Meanwhile, due to the effect of CO layer, the crystallinity (χ_c) of PLA matrix in PLA/HGST3/CO (65/30/5) ternary blends was increased up to 13.1% and the crystallization time was significantly decreased in contrast with PLA/starch/CO (65/30/5). Mechanical properties of PLA/CO/HGSTs (65/5/30) increased markedly compared to the PLA/starch/CO (65/30/5) ternary blend. Therefore, the location of CO molecules has much effect on the properties of resulted blends.

Appendix A. Supplementary data

Supplementary data associated with this article can be found, in the online version, at http://dx.doi.org/10.1016/j.carbpol.2013.01.038.

References

Anderson, K. S., Schreck, K. M., & Hillmyer, M. A. (2008). Toughening polylactide. *Polymer Review*, *48*, 85–108.
Auras, R., Harte, B., & Selke, S. (2004). An overview of polylactides as packaging materials. *Macromolecular Bioscience*, *4*, 835–864.
Bhardwaj, R., & Mohanty, A. K. (2007). Advances in the properties of polylactides based materials: A review. *Journal of Biobased Materials and Bioenergy*, *1*, 191–209.
Bledzki, A. K., & Sperber, V. E. (1999). Recent developments in wood-filled plastics: United States, Japan, and Europe. In *The Fifth International Conference on Woodfiber-Plastics Composites* (pp. 187–192).
Chang, K., Robertson, M. L., & Hillmyer, M. A. (2009). Phase inversion in polylactide/soybean oil blends compatibilized by poly(isoprene-b-lactide) block copolymers. *Applied Material & Interfaces*, *10*, 2390–2399.
Dhital, S., Shrestha, A. K., & Flanagan, B. M. (2010). Cryo-milling of starch granules leads to differential effects on molecular size and conformation. *Carbohydrate Polymers*, *84*, 1133–1140.
Fischer, E. W., Sterzel, H. J., & Wegner, G. (1973). Investigation of structure of solution grown crystals of lactide copolymers by means of chemical-reactions. *Kolloid-zeitschrift and zeitschrift fur polymere*, *251*, 980–990.
Gramlich, W. M., Robertson, M. L., & Hillmyer, M. A. (2010). Reactive compatibilization of poly(L-lactide) and conjugated soybean oil. *Macromolecules*, *43*, 2313–2321.
Guner, F. S., Yagci, Y., & Erciyes, A. T. (2006). Polymers from triglyceride oils. *Progress in Polymer Science*, *31*, 633–670.
Huda, M. S., Drzal, L. T., & Misra, M. (2006). Wood-fiber-reinforced poly(lactic acid) composites: Evaluation of the physicomechanical and morphological properties. *Journal of Applied Polymer Science*, *102*, 4856–4869.
Jacobsen, S., & Fritz, H. G. (1999). Plasticizing polylactide: The effect of different plasticizers on the mechanical properties. *Polymer Engineering and Science*, *39*, 1303–1310.
Jacobsen, S., Fritz, H. G., & Degee, P. (2000). New developments on the ring opening polymerization of polylactide. *Industrial Crops and Products*, *11*, 265–275.
Jiang, W., Yuan, Q., An, L. J., & Jiang, B. Z. (2002). Effect of cavitations on brittle–ductile transition of particle toughened thermoplastics. *Polymer*, *43*, 1555–1558.
Ke, T., & Sun, X. (2003). Thermal and mechanical properties of poly(lactic acid) and starch blends with various plasticizers. *Transactions of the ASAE*, *44*, 945–953.
Lin, Y., Zhang, K. Y., Dong, Z. M., Dong, L. S., & Li, Y. S. (2007). Study of hydrogen-bonded blend of polylactide with biodegradable hyperbranched poly(ester amide). *Macromolecules*, *40*, 6257–6267.
Ma, X. F., Yu, J. G., & Wan, J. J. (2006). Urea and ethanolamine as a mixed plasticizer for thermoplastic starch. *Carbohydrate Polymers*, *64*, 267–273.
Martin, O., & Averous, L. (2001). Poly(lactic acid): Plasticization and properties of biodegradable multiphase systems. *Polymer*, *42*, 6209–6219.
Nayak, P. L. (2000). Grafting of vinyl monomers onto nylon. *Journal of Macromolecular Science-Reviews in Macromolecular Chemistry and Physics*, *C17*, 267–296.
Nijenhuis, A. J., Colstee, E., Grijpma, D. W., & Pennings, A. J. (1996). High molecular weight poly(L-lactide) and poly(ethylene oxide) blends: thermal characterization and physical properties. *Polymer*, *37*, 5849–5857.
Pan, S. J., Guo, R., Peng, J. Y., Chen, Z. M., Liu, H., & Xu, W. J. (2011). A facile method to fabricate hierarchical particulates for superhydrophobic surfaces by diisocyanate reactions. *Journal of Adhesion Science and Technology*, *25*, 1393–1401.
Petrovic, Z. S., Cvetkovic, I., Hong, D. P., Wan, X. M., Zhang, W., Abraham, T., et al. (2008). Polyester polyols and polyurethanes from ricinoleic acid. *Journal of Applied Polymer Science*, *108*, 1184–1190.
Robertson, M. L., Chang, C. K., Gramlich, W. M., & Hillmyer, M. A. (2010). Toughening polylactide with the incorporation of polymerized soybean oil. *Macromolecules*, *43*, 1807–1814.
Robertson, M. L., Paxton, J. M., & Hillmyer, M. A. (2011). Toughened blends of polylactide and castor oil. *Applied Materials & Interfaces*, *3*, 3402–3410.
Rodriguez-Gonzalez, F. J., Ramsay, B. A., & Favis, B. D. (2004). Rheological and thermal properties of thermoplastic starch with high glycerol content. *Carbohydrate Polymers*, *58*, 139–147.
Shi, R., Zhang, Z. Z., Liu, Q. Y., Han, Y. M., Zhang, L. Q., Chen, D. F., et al. (2007). Characterization of citric acid/glycerol co-plasticized thermoplastic starch prepared by melt blending. *Carbohydrate Polymers*, *69*, 748–755.
Sorenson, W. R. (1959). Reaction of an isocyanate and a carboxylic acid in dimethyl sulfoxide. *The Journal of Organic Chemistry*, *24*, 978–980.
Sperling, L. H., & Mishra, V. (1996). The current status of interpenetrating polymer networks. *Polymers for Advanced Technologies*, *7*, 197–208.

Tang, Z. B., Zhang, C. Z., Liu, X. Q., & Zhu, J. (2012). The crystallization behavior and mechanical properties of polylactic acid in the presence of a crystal nucleating agent. *Journal of Applied Polymer Science*, *125*, 1108–1115.

Teixeira, E. M., Da Roz, A. L., Carvalho, A. J. F., & Curvelo, A. A. S. (2007). The effect of glycerol/sugar/water and sugar/water mixtures on the plasticization of thermoplastic cassava starch. *Carbohydrate Polymers*, *69*, 619–624.

Tianyi, K., & Sun, X. Z. (2003). Melting behavior and crystallization kinetics of starch and poly(lactic acid) composites. *Journal of Applied Polymer Science*, *89*, 1203–1210.

Wang, H., Sun, X. Z., & Seib, P. (2001). Strengthening blends of poly(lactic acid) and starch with methylenediphenyl diisocyanate. *Journal of Applied Polymer Science*, *82*, 1761–1767.

Wang, J. W., Zhai, W. T., & Zheng, W. G. (2012). Poly(ethylene glycol) grafted starch introducing a novel interphase in poly(lactic acid)/poly(ethylene glycol)/starch ternary composites. *Journal of Polymer Environment*, *2*, 528–539.

Wu, C. S. (2005). Improving polylactide/starch biocomposites by grafting polylactide with acrylic acid—characterization and biodegradability assessment. *Macromolecular Bioscience*, *5*, 352–361.

Xie, F. W., Xue, T., Yu, L., Chen, L., Li, X. X., Zhang, X. M., et al. (2007). Rheological properties of starch-based materials and starch/poly(lactic acid) blends. *Macromolecular Symposia*, *249/250*, 529–534.

Xing, Q., Zhang, X. Q., Dong, X., Liu, G. M., & Wang, D. J. (2012). Low-molecular weight aliphatic amides as nucleating agents for poly(L-lactic acid): Conformation variation induced crystallization enhancement. *Polymer*, *53*, 2306–2314.

Xiong, Z., Yang, Y., Feng, J. X., Zhang, X. M., Zhang, C. Z., Tang, Z. B., et al. (2013). Preparation and characterization of poly(lactic acid)/starch composites toughened with epoxidized soybean oil. *Carbohydrate Polymers*, *92*, 810–816.

Yu, L., Petinakis, E., Dean, K., Liu, H. S., & Yuan, Q. A. (2011). Enhancing compatibilizer function by controlled distribution in hydrophobic polylactic acid/hydrophilic starch blends. *Journal of Applied Polymer Science*, *119*, 2189–2195.

Zhang, J. F., & Sun, X. Z. (2004). Mechanical properties of poly(lactic acid)/starch composites compatibilized by maleic anhydride. *Biomacromolecules*, *5*, 1446–1451.

Zhong, W., Ge, J. J., Gu, Z. Y., Chen, X., Zhang, Y., Yang, Y. L., et al. (1999). Study on biodegradable polymer materials based on poly(lactic acid). I. Chain extending of low molecular weight poly(lactic acid) with methylenediphenyl diisocyanate. *Journal of Applied Polymer Science*, *74*, 2546–2551.